

Optimal operation of reactive simulated moving bed and Varicol systems[†]

Weifang Yu, K Hidajat and Ajay K Ray*

Department of Chemical and Environmental Engineering, National University of Singapore, 10 Kent Ridge Crescent, Singapore 119260

Abstract: In this article, the performance of a reactive Simulated Moving Bed (SMB) and its modification, the more flexible Varicol process, is improved for the synthesis of methyl acetate (MeOAc) ester by multi-objective optimization using Non-dominated Sorting Genetic Algorithm (NSGA). The Varicol process is based on a non-synchronous shift of the inlet and outlet ports instead of the synchronous one used in the traditional SMB technology. The optimization problems considered are both two- and three-objective function problems. In one case, optimization was aimed at simultaneous maximization of the purity of MeOAc and minimization of adsorbent (and catalyst) requirement for the reactive SMB; while in the other case, maximization of purity and yield of MeOAc together with minimization of eluent (methanol) consumption for both reactive SMB and Varicol systems were considered. When the optimal solutions were compared, it was found that reactive Varicol systems could produce a higher purity product for a fixed yield, and consume slightly less eluent in the high purity region than more rigid SMB systems.

© 2003 Society of Chemical Industry

Keywords: multi-objective optimization; simulated moving bed; reactive separation; genetic algorithm; multi-functional reactor

NOTATION

d_{col}	Diameter of column
L	Length of column
N_{col}	Total number of columns
Q	Volumetric flow rate
t_s	Switching time
Y	Yield
α	Ratio of feed flow rate to flow rate in section P
β	Ratio of raffinate flow rate to flow rate in section P
γ	Ratio of eluent flow rate to flow rate in section P

INTRODUCTION

Simulated Moving Bed (SMB)¹ systems are used for separations that are either impossible or difficult using traditional separation techniques. By virtue of its superior separating power, the SMB system has become one of the most popular technologies, finding application in the petrochemical and sugar industries; and of late, there has been a dramatic increase in interest in SMB in the pharmaceutical industry for enantio-separations.² SMB systems can also be integrated to include reactions^{3,4} which can provide

economic benefit for equilibrium-limited reversible reactions, such as many hydrogenation, isomerization, and esterification reactions. *In-situ* separation of the products allows the reversible reaction to proceed to completion beyond the thermodynamic equilibrium and at the same time products of high purity to be obtained. The recently developed Varicol process⁵ is based on the non-synchronous shift of the inlet and outlet ports during a global switching period instead of the synchronous one used in the SMB technology. The successful implementation of reactive SMB and Varicol processes on an industrial scale will necessitate the optimal design parameters and operating conditions to be determined. Several studies^{6–8} have reported on the design and optimization of reactive SMB, but they only involve a single objective optimization in terms of productivity, which is usually not sufficient for the real-life complex design, since operating variables often influence the performance of reactive SMB in conflicting ways. Hence, multi-objective optimization⁹ is essential for the design of reactive SMB and Varicol systems.

The principle of multi-criterion optimization with conflicting objectives is different from that of single objective optimization. Instead of trying to find the best design (unique global) solution, the goal of multi-objective optimization is to obtain a set of equally good non-dominated solutions, which are known as Pareto

* Correspondence to: Ajay K Ray, Department of Chemical and Environmental Engineering, National University of Singapore, 10 Kent Ridge Crescent, Singapore 119260

E-mail: cheakr@nus.edu.sg

[†] Paper presented at the Process Innovation and Process Intensification Conference, 8–13 September 2002, Edinburgh, UK (Received 15 April 2002; revised version received 10 October 2002; accepted 17 October 2002)

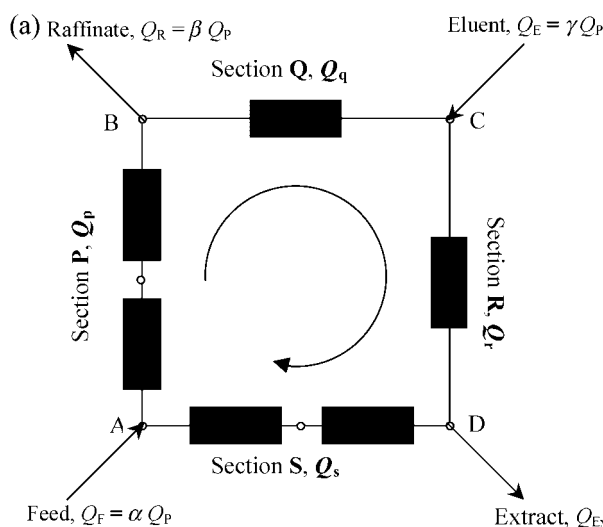
optimal solutions. In a set of Pareto solutions, no solution could be considered better than other solutions with respect to all objective functions.

In this work, multi-objective optimization has been performed for the synthesis of methyl acetate (MeOAc) in reactive SMB and Varicol systems using Non-dominated Sorting Genetic Algorithm (NSGA).¹⁰ To the best of our knowledge, this is the first attempt to extend the concept of the Varicol (variable column) process to reactive systems, and compare the optimal solutions with those of reactive SMB. The objectives of this paper are to deepen the understanding of reactive SMB and Varicol processes and provide a new approach toward their optimal design.

SIMULATED MOVING BED (SMB) SYSTEM AND VARICOL PROCESS

In an SMB system, a fixed bed is used, and successive switching of the feed and product positions at timed intervals simulates the movement of the solid.^{3,4} The solid phase velocity can be defined as the ratio of the column length and the switching time.¹¹ One obvious shortcoming of the SMB operating mode is that the velocity of the solid is constant in all sections as constant values of both switching time and length are used. Recently, a novel process, Varicol,⁵ which is based on non-simultaneous and unequal shifts of the inlet/outlet ports, has been developed. The concept and the principle of operation for a four-subinterval Varicol process together with the equivalent SMB process are illustrated schematically in Fig 1 for one switching period. Figure 1(a) shows a schematic diagram of a six-column SMB and the principle of its operation. It consists of columns of uniform cross-section, each of length L and packed with an adsorbent. The columns are connected in series in a circular array. Two incoming fluid streams (feed and eluent) and two outgoing fluid streams (extract and raffinate) divide the system into four sections, with two, one, one and two columns in each section respectively, corresponding to the column configuration 2/1/1/2. Simulation of countercurrent movement of the solid and the fluid is achieved by advancing the inlet and withdrawal ports, column by column, in the same direction as the fluid flow, at a predetermined switching time, t_s . Switching time and column configuration (the number of columns in each section) in SMB processes are usually decided *a priori* and remain constant during the entire operation.

In contrast to SMB, the Varicol process is based on a non-simultaneous and unequal shift of the inlet/outlet ports. The concept and the principle of operation of the Varicol process together with the equivalent SMB process are illustrated schematically in Fig 1(b) for one switching period. The switching time, t_s , which is related directly to the solid flow rate in SMB, is also a key parameter in the Varicol process, although the relationship is not straightforward. In Varicol opera-



P, Q, R, S: four sections divided by feed and withdrawal ports; p, q, r, s: number of columns in section P, Q, R, S; Q_F, Q_R, Q_E, Q_{Ex} : flow rate of feed, raffinate, eluent, extract; Q_p, Q_q, Q_r, Q_s : flow rate in section P, Q, R, S, $Q_q = Q_p(1-\beta)$, $Q_r = Q_p(1-\beta+\gamma)$, $Q_s = Q_p(1-\alpha)$, where α, β, γ : $Q_F/Q_p, Q_R/Q_p, Q_E/Q_p$; L : length of each column; t_s : time interval between two successive switchings.

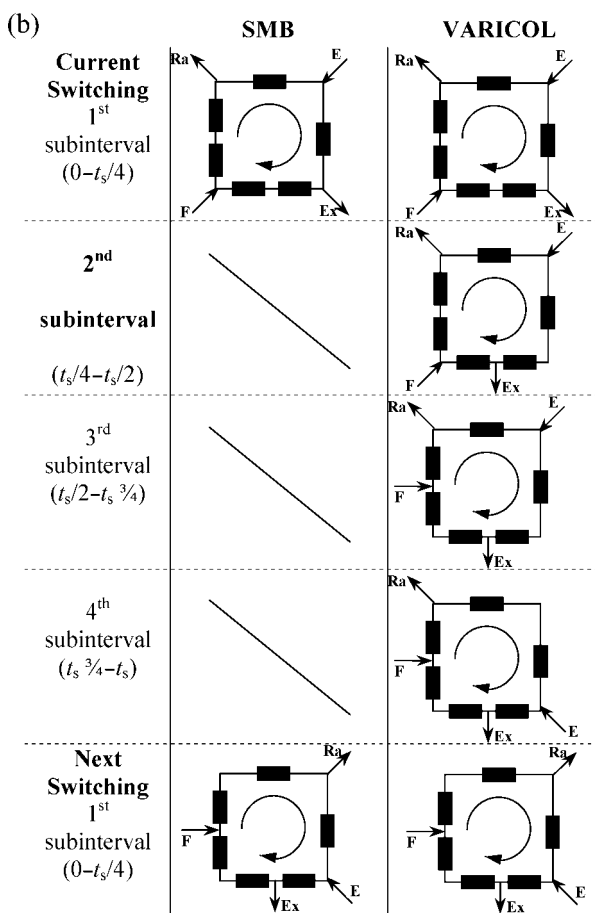


Figure 1. (a) Schematic diagram of a six-column SMB system. (b) Principle of operation of SMB and four-subinterval Varicol system (port switching schedule).

tion, a non-synchronous shift of the inlet and outlet ports is usually employed within a switching period, which is again kept constant in time. This is shown as an illustrative example in Fig 1(b) for a four-

subinterval Varicol process. Within one (global) switching period t_s , the column configuration changes from 2/1/1/2 ($0-t_s/4$) to 2/1/2/1 ($t_s/4-t_s/2$) by shifting the extract port forward by one column, then to 1/1/2/2 ($t_s/2-t_s/3/4$) by shifting the feed port one column forward, then to 1/2/1/2 ($t_s/3/4-t_s$) by shifting the eluent port one column forward, and finally return to the original configuration of 2/1/1/2 by shifting the raffinate port one column forward. As a result, in a four-subinterval Varicol process, there are four different column configurations for the four subintervals due to local switching during one global switching period. The number of columns in each zone varies with time within a global switching period, but the number of columns in each zone returns to the starting value at the end of the global switching period. In terms of average number of columns per zone this corresponds to the configuration 1.5/1.25/1.5/1.75. Note that the average number for any particular zone is obtained as follows: for example, for zone P, 1.5 is obtained from $(2+2+1+1)/4$, where the numbers in parenthesis are the number of columns in zone P in the four subintervals.

Therefore, locations of input/output ports in Varicol processes are quite different from SMB processes. Note that in principle it is possible that a port may shift more than once during one global switching period, either forward or even in a backward direction. As a result, Varicol processes can have several column configurations, which endow more flexibility compared with SMB processes. SMB processes can be regarded as a special case of the more flexible Varicol processes. It is notable that the Varicol process does not add any additional fixed cost.

MATHEMATICAL MODEL

The direct synthesis of methyl acetate ester (MeOAc) from methanol (MeOH) and acetic acid (HOAc) catalysed by Amberlyst 15 ion exchange resin has been considered as an example. The mathematical model reported by Zhang *et al*¹² was adopted to describe the dynamic behaviour of reactive SMB and Varicol systems except that the reaction rate is given by:

$$R_j^{(N)} = k_f \left[q_{\text{HOAc},j}^{(N)} - \frac{q_{\text{MeOAc},j}^{(N)} \cdot q_{\text{H}_2\text{O},j}^{(N)}}{K_e} \right] \quad (1)$$

The kinetic, adsorption constants and diffusion coefficients of each component involved in the process were determined semi-empirically by fitting the experimentally measured breakthrough curves with the model prediction obtained by solving the mass balance equation given by:

$$\frac{\partial C_i}{\partial t} + \left(\frac{1-\varepsilon}{\varepsilon} \right) \frac{\partial q_i}{\partial t} + \frac{u}{\varepsilon} \frac{\partial C_i}{\partial z} - \left(\frac{1-\varepsilon}{\varepsilon} \right) v_i R = D_i \frac{\partial^2 C_i}{\partial z^2} \quad (2)$$

$$\text{where } q_i = K_i C_i \quad (3)$$

The initial and boundary conditions are:

$$C_i[t = 0] = C_i^0 \quad (4)$$

$$C_i[0 < t < t_p]_{z=0} = C_{f,i} \quad (5)$$

$$C_i[t > t_p]_{z=0} = 0 \quad (6)$$

$$\left[\frac{\partial C_i(t)}{\partial z} \right]_{z=0} = 0 \quad (7)$$

At 318K, the values obtained are $K_{\text{HOAc}}=0.425$, $K_{\text{MeOAc}}=0.376$, $K_{\text{H}_2\text{O}}=2.938$; $D_{\text{HOAc}}=3.884 \text{ m}^2 \text{ s}^{-1}$, $D_{\text{MeOAc}}=3.884 \text{ m}^2 \text{ s}^{-1}$, $D_{\text{H}_2\text{O}}=11.168 \text{ m}^2 \text{ s}^{-1}$; $k_f=1.062 \text{ min}^{-1}$ and $K_e=334.023 \text{ mol dm}^{-3}$. Detailed procedures are described elsewhere.¹³ The partial differential equations were solved using the Method of Lines and were first discretized in space using the Finite Difference Method (FDM) to convert them into a set of several-coupled Ordinary Differential Equation-Initial Value Problems (ODE-IVPs) and the resultant stiff ODEs of the initial value kind were solved using the subroutine, DIVPAG, in the IMSL library.

MULTI-OBJECTIVE OPTIMIZATION

In single objective function optimization, one attempts to find the best design, which is usually the global minimum (or maximum). However, most real world problems involve the simultaneous optimization of multiple objective functions (a vector). Such problems are conceptually different from single objective function problems. In multiple objective function optimization, there may not exist a solution that is the best (global optimum) with respect to all objectives. Instead, there *could* exist an entire set of optimal solutions that are *equally* good. These solutions are known as Pareto-optimal (or non-dominated) solutions. A Pareto set, for example, for a two objective function problem is described by a set of points such that when one moves from one point to any other, one objective function improves, while the other worsens. Thus, one cannot say that any one of these points is superior (or dominant) to any other. Since none of the non-dominated solutions in the Pareto set is superior to any other, any one of them is an acceptable solution. The choice of one solution over the other requires additional knowledge of the problem, and often this knowledge is intuitive and non-quantifiable. In the present study, work on the multiobjective optimization for a chemical process as complex as the reactive SMB and Varicol processes is reported. For proper design of a reactive SMB, and more importantly, understanding the principle of operation of a reactive SMB, a multi-objective optimization study is much more meaningful.

Case 1. Maximization of purity of MeOAc (P_{MeOAc}) and minimization of volume of solid (V_{solid})

The performance of a reactive SMB was first

optimized at the design stage to determine the optimal length of column to minimize the total amount of adsorbent (V_{solid}) required while at the same time producing as high purity product as possible. It is described mathematically as:

$$\text{Maximize } \mathcal{J}_1 = P_{\text{MeOAc}}(t_s, L, \gamma) \quad (8)$$

$$\text{Minimize } \mathcal{J}_2 = V_{\text{solid}}(t_s, L, \gamma) \quad (9)$$

Subject to

$$P_{\text{MeOAc}} \geq 80\%; Y_{\text{MeOAc}} \geq 80\% \quad (10)$$

$$1(\text{min}) \leq t_s \leq 40(\text{min}); 10\text{cm} \leq L \leq 100\text{cm}; \\ 1 \leq \gamma \leq 2.5 \quad (11)$$

for fixed values of $Q_p = 2 \text{ cm}^3 \text{ min}^{-1}$; $\alpha = 0.1$; $\beta = 0.6$; $d_{\text{col}} = 0.94 \text{ cm}$; $N_{\text{col}} = 4$; $C_{\text{HOAc}}^{\text{feed}} = 2 \text{ mol dm}^{-3}$. The modified objective functions incorporating the inequality constraints as penalty functions are written as:

$$\text{Minimize } I_1 = 1/(1 + \mathcal{J}_1) + w(f_1 + f_2)$$

$$\text{Minimize } I_2 = \mathcal{J}_2 + w(f_1 + f_2)$$

where:

$$f_1 = |P_{\text{MeOAc}} - 0.80| - (P_{\text{MeOAc}} - 0.80)$$

$$f_2 = |Y_{\text{MeOAc}} - 0.80| - (Y_{\text{MeOAc}} - 0.80)$$

The penalty value (w) was given as 10^3 for all the

optimization problems discussed in this article to ensure the fulfilling of the constraints. A non-dominated sorting genetic algorithm (NSGA)^{9,10} was used with the model described above to optimize the reactive SMB and Varicol processes. NSGA generates a set of solutions that are non-dominating over each other, and constitute multi-objective Pareto optimal solutions representing optimal operating conditions for the SMB and Varicol processes. Indeed, NSGA has been applied recently to optimize several industrially important processes in chemical engineering, including an industrial nylon-6 semi-batch reactor,¹⁴ a wiped-film polyester reactor,¹⁵ PMMA film reactor,¹⁶ a steam reformer,¹⁷ hydrogen plant,¹⁸ beer dialysis,¹⁹ cyclone separators,²⁰ Venturi scrubber,²¹ MTBE synthesis in SMBR,²² and a styrene reactor.²³

RESULTS AND DISCUSSION

The Pareto optimal solution and corresponding decision variables are shown in Fig 2 for case 1. Figure 2(a) shows that the purity of MeOAc increases at the cost of increasing adsorbent requirement. From Fig 2(b), it can be observed that the eluent flow rate tends to reach the upper boundary, especially in the high purity region. This is due to the fact that high desorbent flow rate in section R leads to complete regeneration of adsorbent, which in turn improves product purity. Figure 2(c and d) also shows that an

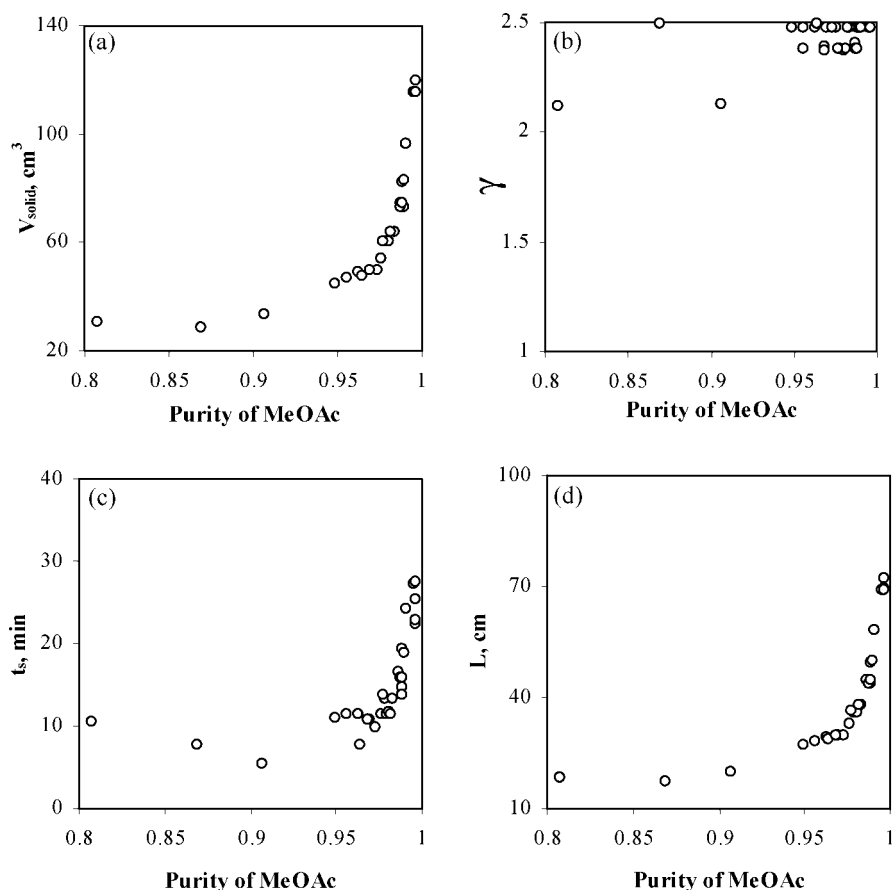


Figure 2. Pareto optimal solutions and corresponding values of decision variables for case 1 optimization problem. (a) Effect of volume of adsorbent; (b) effect of eluent flow rate; (c) effect of switching time; (d) effect of column length.

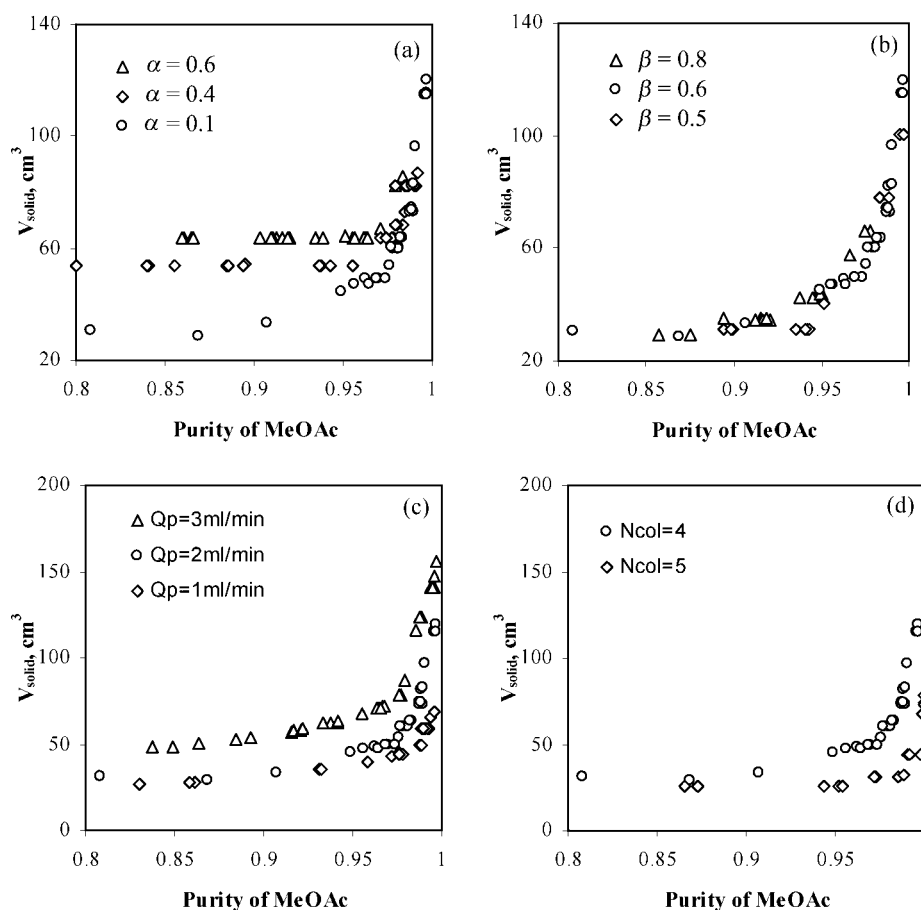


Figure 3. Effect of various parameters on the Pareto optimal solutions; (a) effect of feed flow rate, α , (b) effect of raffinate flow rate, β , (c) effect of column flow rate, Q_p , and (d) effect of number of columns, N_{col} .

optimal switching time corresponding to a specific length of column exists.

Effect of feed flow rate, α

The effect of feed flow rate on the Pareto was investigated by comparing the optimal solutions for α at 0.1, 0.4 and 0.6. It is shown in Fig 3(a) that more adsorbent is needed to achieve the same purity requirement as α increases. When Q_p is kept constant, increase of α leads to the decrease of Q_s , which deteriorates the performance of section S, since it is responsible for desorbing MeOAc. Hence, t_s has to be increased to improve the performance of section S due to the constraint on yield. However, the increase of t_s is not desirable for section P, since water will break through and decrease P_{MeOAc} in the raffinate stream. Hence, for same purity requirement, the length of column has to be increased to retain water from breaking through in section P.

Effect of raffinate flow rate, β

Figure 3(b) shows the shift of Pareto for different values of β . It can be seen that the adsorbent requirement slightly increases as β increases to obtain the same purity of product. When β increases, both Q_q and Q_r decrease while Q_E can be assumed to be constant, as it tends to reach the upper boundary. The decrease of Q_q is favourable, since the role of section Q is to clean the solvent for recycling. However, the

decrease in Q_r will deteriorate the complete regeneration of the resin. So t_s has to be increased to improve the performance of section R, otherwise the remaining water in the adsorbent will later pollute the product ester in the raffinate stream. Again, as discussed above, the length of column has to be increased to prevent water breaking through in section P.

Effect of flow rate in section P, Q_p

As shown by Fig 3(c), the adsorbent requirement increases for the same product purity as Q_p increases. This is due to the fact that the length of each column has to be increased to provide sufficient residence time to allow the reaction to proceed, since unconverted acetic acid will primarily leave with ester product at the raffinate port due to their similar adsorption affinity toward the solid adsorbent, thereby contaminating the purity of the ester in the raffinate stream if conversion is kept low.

Effect of total number of columns, N_{col}

Figure 3(d) shows the comparison of Pareto optimal solutions for different total number of columns. It is found that the adsorbent requirement for a five-column unit is less than that of a four-column unit for the same purity requirement. This is due to the fact that the minimum length of column required to achieve the same product purity becomes smaller, since each section of the SMB plays a specific role in

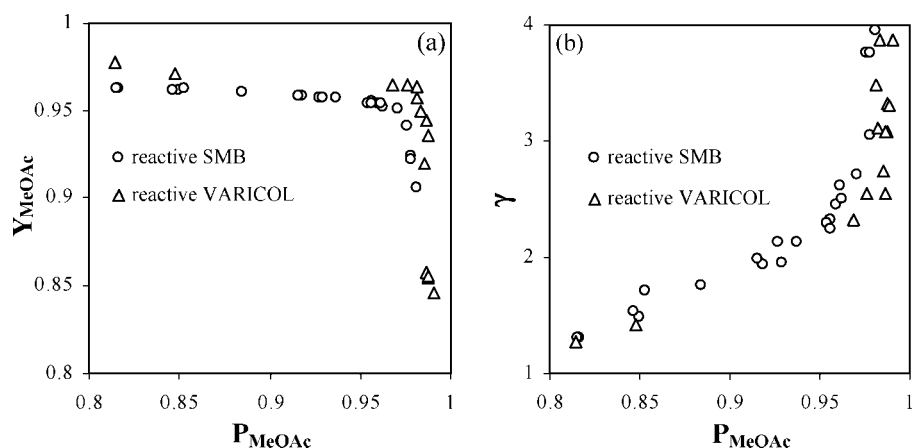


Figure 4. Comparison of Pareto optimal solutions between reactive SMB and Varicol systems.

achieving the separation of reaction products. Sections P and S are primarily responsible for retention of the strongly adsorbed component (water). The functions of sections Q and R are to clean the solvent and regenerate the columns by desorbing the strongly adsorbed component. For the objective function of maximization of P_{MeOAc} , the roles of section Q and section R are less important. Reactive sections primarily control the minimum length of column and therefore, by introducing one more column into the reactive section (section P), the minimum length of each column could be reduced to achieve the same product purity. The optimal (minimum) lengths of each column obtained were 17 cm and 10 cm respectively for a four-column and a five-column SMB unit.

Case 2. Maximization of purity and yield of MeOAc and minimization of eluent consumption

In this section, the performance of both reactive SMB and Varicol processes were optimized for an existing unit. The length of column was fixed as 10 cm based on the results of five-column optimal solutions in case 1. The problem is described mathematically as follows:

$$\text{Maximize } I_1 = P_{\text{MeOAc}}(t_s, \beta, \gamma) \quad (12)$$

$$\text{Maximize } I_2 = Y_{\text{MeOAc}}(t_s, \beta, \gamma) \quad (13)$$

$$\text{Minimize } I_3 = \gamma(t_s, \beta, \gamma) \quad (14)$$

Subject to

$$P_{\text{MeOAc}} \geq 80\%; Y_{\text{MeOAc}} \geq 80\% \quad (15)$$

$$1(\text{min}) \leq t_s \leq 20(\text{min}); 1 \leq \gamma \leq 4; 0.1 \leq \beta \leq 0.9 \quad (16)$$

$$Q_p = 2 \text{ cm}^3 \text{ min}^{-1}; \alpha = 0.1; d_{\text{col}} = 0.94 \text{ cm}; N_{\text{col}} = 5; L = 10 \text{ cm}; C_{\text{HOAc}}^{\text{feed}} = 2 \text{ mol dm}^{-3} \quad (17)$$

For the convenience of analysis, the Pareto solutions were plotted in two dimensions, that is, Y_{MeOAc} or γ against P_{MeOAc} . Figure 4(a) shows that P_{MeOAc} decreases as Y_{MeOAc} increases for both reactive SMB and Varicol systems and the performance of Varicol is better than

that of SMB in terms of higher yield for the same purity requirement. From Fig 4(b), it can be observed that the increase of P_{MeOAc} is at the cost of eluent consumption (γ) for both reactive SMB and Varicol systems and the γ is lower for Varicol than that for SMB for the same purity requirement, especially in the high purity region. The optimal column distribution for Varicol was found to be 1-1-1-2, 2-1-1-1, 2-1-1-1 for the four-subintervals. The optimal switching time, t_s , obtained was 3.5 min and 2.9 min respectively for the SMB and the Varicol system. The better performance of the Varicol system results in its flexibility in column distribution, leading to better utilization of adsorbent.

CONCLUSIONS

The multi-objective optimization of reactive SMB and Varicol systems were performed using NSGA for the synthesis of MeOAc. The effects of flow rates and total number of columns on the performance of reactive SMB were investigated. It was found that the performance of reactive the Varicol system could be better than that of the reactive SMB system due to increased flexibility.

REFERENCES

- 1 Magee EM, Canadian Patent No 631 882 (1961).
- 2 Zhang Z, Hidajat K, Morbidelli M and Ray AK, Multi-objective optimization of SMB and Varicol process for chiral Separation. *AIChE J* **48**(12):2800–2816 (2002).
- 3 Ray AK, Carr RW and Aris R, The simulated countercurrent moving bed chromatographic reactor: a novel reactor–separator. *Chem Engg Sci* **49**(4):469–480 (1994).
- 4 Ray AK and Carr R, Experimental study of a laboratory scale simulated countercurrent moving bed chromatographic reactor. *Chem Engg Sci* **50**(14):2195–2202 (1995).
- 5 Ludemann-Hombourger O, Nicoud RM and Bailly M, The Varicol process: a new multi-column continuous chromatographic process. *Sep Sci Technol* **35**(12):1829–1862 (2000).
- 6 Migliorini C, Fillinger M, Mazzotti M and Morbidelli M, Analysis of simulated moving bed reactors. *Chem Engg Sci* **54**:2475–2480 (1999).
- 7 Diana CS and Rodrigues AE, Design methodology and operation of a simulated moving bed reactor for the inversion of sucrose and glucose–fructose separation. *Chem Engg Sci* **82**:95–107 (2001).

- 8 Lode F, Houmar M, Migliorini C, Mazzotti M and Morbidelli M, Continuous reactive chromatography. *Chem Engg Sci* **56**:269–291 (2001).
- 9 Bhaskar V, Gupta SK and Ray AK, Applications of multi-objective optimization in chemical engineering. *Rev Chem Engg* **16**:1–54 (2000).
- 10 Deb K, *Multi-Objective Optimization using Evolutionary Algorithms*, John Wiley & Sons, Chichester, UK (2001).
- 11 Ray AK, Tonkovich A, Carr RW and Aris R, The simulated countercurrent moving bed chromatographic reactor: a novel reactor–separator. *Chem Engg Sci* **45**(8):2431–2437 (1990).
- 12 Zhang Z, Hidajat K and Ray AK, Application of simulated moving-bed chromatographic reactor for MTBE synthesis. *Ind Eng Chem Res* **40**(23):5305–5316 (2001).
- 13 Yu W, Hidajat K and Ray AK, Determination of adsorption and kinetic parameters for methyl acetate synthesis reaction in Amberlyst 15 ion exchange resin. *Applied Catalysis A: General* (2002) (submitted).
- 14 Mitra K, Deb K and Gupta SK, Multiobjective dynamic optimization of an industrial Nylon 6 semibatch reactor using genetic algorithm. *J Appl Polym Sci* **69**:69 (1998).
- 15 Bhaskar V, Gupta SK and Ray AK, Multiobjective optimization of an industrial wiped film poly(ethylene terephthalate) reactor. *AIChE J* **46**(5):1046 (2000).
- 16 Zhou F, Gupta SK and Ray AK, Multiobjective optimization of the continuous casting process for PMMA using adapted genetic algorithm. *J Appl Polym Sci* **78**:1439 (2000).
- 17 Rajesh JK, Gupta SK, Rangaiah GP and Ray AK, Multiobjective optimization of steam reformer performance using genetic algorithm. *Ind Eng Chem Res* **39**(3):706 (2000).
- 18 Rajesh JK, Gupta SK, Rangaiah GP and Ray AK, Multi-objective optimization of industrial hydrogen plants. *Chem Engg Sci* **56**(3):999 (2001).
- 19 Yuen CC, Aatmeeyata, Gupta SK and Ray AK, Multi-objective optimization of membrane separation modules using genetic algorithm. *J Membrane Sci* **176**(2):177 (2000).
- 20 Ravi G, Gupta SK and Ray MB, Multiobjective optimization of cyclone separators. *Ind Eng Chem Res* **39**(11):4272 (2000).
- 21 Ravi G, Gupta SK, Viswanathan S and Ray MB, Optimization of venture scrubbers using genetic algorithm. *Ind Eng Chem Res* **41**(12):2988–3002 (2002).
- 22 Zhang Z, Hidajat K and Ray AK, Multiobjective optimization of simulated countercurrent moving bed chromatographic reactor for MTBE synthesis. *Ind Eng Chem Res* **41**:3213–3232 (2002).
- 23 Yee AKY, Ray AK and Rangaiah GP, Multiobjective optimization of an industrial styrene reactor. *Comp Chem Engg* (in press) (2002).